5441

Copy 1

A Biomimetic Propulsor for Active Noise Control: Experiments

Promode R. Bandyopadhyay
NUWC Division Newport and Office of Naval Research

William P. Krol Jr.
Daniel P. Thivierge
William H. Nedderman
NUWC Division Newport

Mehran Mojarrad
Biomimetics Products Inc.

NAVSEA
NEWPORT
Undersea Warfare Center Division

Naval Undersea Warfare Center Division
Newport, Rhode Island

011351   001N

PREFACE

This report was funded by the Office of Naval Research Cognitive & Neural Sciences Program, program officer Teresa McMullen.

The technical reviewer for this report was James L. Dick (Code 8233).

Reviewed and Approved: 1 March 2002

Paul M. Dunn
Head, Weapon Systems Technology Department

REPORT DOCUMENTATION PAGE

Form Approved
OMB No. 0704-0188

1. AGENCY USE ONLY *(Leave blank)*	2. REPORT DATE 1 March 2002	3. REPORT TYPE AND DATES COVERED

4. TITLE AND SUBTITLE

A Biomimetic Propulsor for Active Noise Control: Experiments

5. FUNDING NUMBERS

6. AUTHOR(S)

Promode R. Bandyopadhyay, William P. Krol Jr., Daniel P. Thivierge, William H. Nedderman, Mehran Mojarrad

7. PERFORMING ORGANIZATION NAME(S) AND ADDRESS(ES)

Naval Undersea Warfare Center Division
1176 Howell Street
Newport, RI 02841-1708

8. PERFORMING ORGANIZATION REPORT NUMBER

TR 11,351

9. SPONSORING/MONITORING AGENCY NAME(S) AND ADDRESS(ES)

Office of Naval Research
800 North Quincy Street
Arlington, VA 22217-5660

10. SPONSORING/MONITORING AGENCY REPORT NUMBER

11. SUPPLEMENTARY NOTES

12a. DISTRIBUTION/AVAILABILITY STATEMENT

Approved for public release; distribution is unlimited.

12b. DISTRIBUTION CODE

13. ABSTRACT (Maximum 200 words)

A strategy for the reduction of radiated noise of underwater propulsors has been developed by means of modeling. It requires a means for blade lift enhancement, which allows a lowering of the rotational speed of the propulsor. Laboratory experiments have been carried out with small propulsor models to demonstrate a biomimetic actuator technology for cambering blades actively for lift enhancement. Propulsor blades are constructed partially out of lightweight, electroactive polymeric sheets, also known as artificial muscles. The blade motion is digitally controlled and can be complex. Active lift enhancement is demonstrated.

14. SUBJECT TERMS
Underwater Propulsion   Hydrodynamics   Underwater Sound

Biomimetics   Biorobotics   Biology-Inspired Propulsion   Artificial Muscles

15. NUMBER OF PAGES
29

16. PRICE CODE

17. SECURITY CLASSIFICATION OF REPORT Unclassified	18. SECURITY CLASSIFICATION OF THIS PAGE Unclassified	19. SECURITY CLASSIFICATION OF ABSTRACT Unclassified	20. LIMITATION OF ABSTRACT SAR

NSN 7540-01-280-5500

Standard Form 298 (Rev. 2-89)
Prescribed by ANSI Std. Z39-18
298-102

TABLE OF CONTENTS

LIST OF ILLUSTRATIONS

A BIOMIMETIC PROPULSOR FOR
ACTIVE NOISE CONTROL: EXPERIMENTS

1. INTRODUCTION

The broad subject of this report entails the process of making small underwater bodies quieter. The process begins with the assumption that the acts of flying and swimming in nature hold the key to new advances in stealth. This assumption may be based on unsteady hydrodynamic or acoustic mechanisms special to the species, or an enhancement in the performance of the former leading to gains in the latter. For example, Ellington[1] and Dickinson et al.[2] have shown that the flight of a fruit fly, which defies conventional steady-state aerodynamics, is made possible by the presence of two unsteady rotational aerodynamic mechanisms, in additional to the conventional translational mechanism. The experimentation presented in this report provides the groundwork for future consideration of these mechanisms in building new kinds of biologically inspired propulsor blades. For the successful application of these blades, a bridge must be built between the distilled advances in locomotive biology and appropriately chosen applications. Over the past few years, the Naval Undersea Warfare Center (NUWC) Division, Newport, RI, has been engaged in such bridge building.[3-8]

This report is concerned with building a case for the development of a new strategy in the reduction of noise in small underwater vehicles. Modeling is carried out in section 2 to broadly outline this approach. A key component of this strategy is then demonstrated experimentally and is described in section 3. A small biomimetic propulsor, with blades made of artificial muscles, was built and demonstrated for this experiment. These electroactive muscles have several appealing features. They are quiet in operation because they require no vibration-causing motors, gears, or shafting to operate; this is an attractive feature for small underwater vehicles where space is at a premium. Also, these actuators are amenable to digital electronics and programming, which make them suitable for active control.

2. RADIATED NOISE REDUCTION STRATEGY

Recent understanding of the mechanism of lift production by fruit flies suggests that they have three submechanisms involved, namely, delayed stall, rotational circulation, and wake capture.[1,2] The first is a translational mechanism, while the last two involve unsteady hydrodynamics involving a rotation of the blade, which is absent in common man-made lifting surfaces such as aircraft wings, or blades of rotating fluid machineries such as propulsors, helicopter rotors, pumps, compressors, and turbines. At NUWC Division Newport, the question of how to incorporate these additional unsteady mechanisms into the blades of the propulsor

of a small underwater vehicle is examined. The task is not easy because a blade rotation is needed. However, the availability of certain emerging material technologies suggests that the manufacture of dynamically moving blades might be feasible. This report is concerned with demonstrating that this is a fruitful path to explore for lift enhancement. The modeling described below was conceived to determine the potential impact of such lift enhancement on stealth.

The details of the modeling of the radiated noise are given in the appendix. The result is shown in figure 1, which shows the reduction in radiated noise due to a reduction in the rotational speed (measured in revolutions per minute (rpm)) of the propulsor. Other than cavitation, three sources of noise are considered, namely blade rate tonals due to wake deficits, trailing edge singing, and the effect of turbulence ingested from upstream; these are approximately described by functions proportional to velocity to the 4th, 5th, and 6th powers,[9] respectively. Observe that an rpm reduction of 10% can lead to a noise reduction of 3–5 dB, which is significant. This is the origin of the strategy proposed in this report: that an rpm reduction should be sought via enhanced blade lift whereby the forward speed remains unchanged.
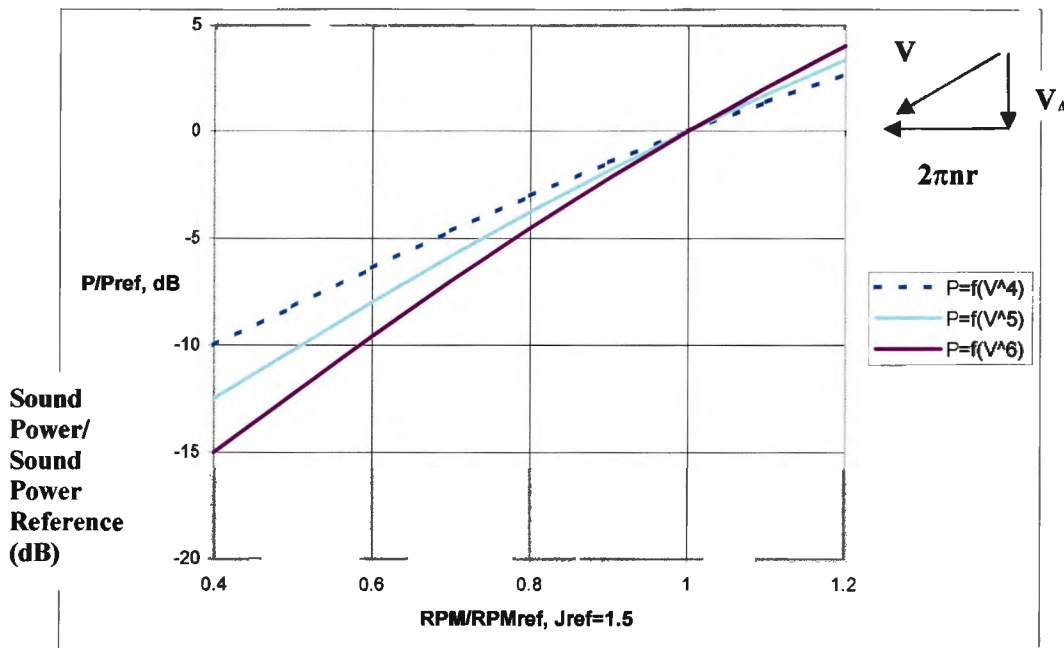
Figure 1. Modeling of the Effect of Rotational Speed Reduction on Radiated Noise

3. BIOMIMETIC PROPULSOR

A propulsor provides thrust to an underwater vehicle. In this section, an experiment on a small propulsor with two biomimetic blades, incorporating an emerging electro-active material technology, is described. The entire experiment is described in a video.[8]
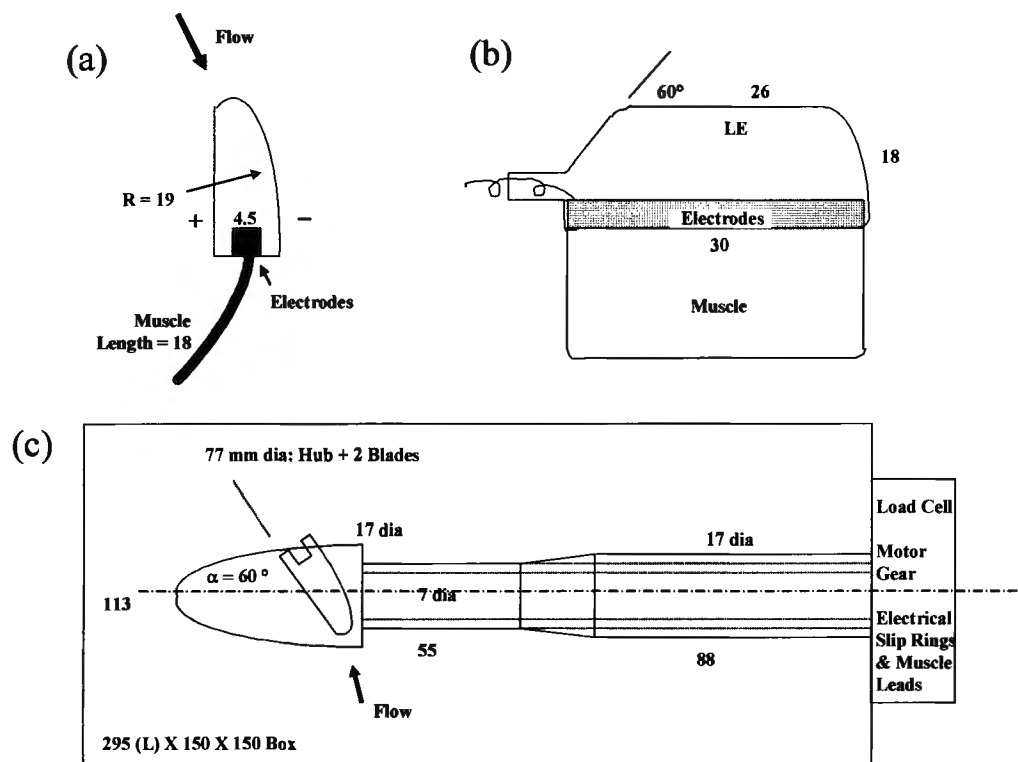
3.1   BIOMIMETIC BLADES

Figure 2 shows the propulsor blades schematically. As shown in figure 2(a), the blades have a rigid forward part and an artificial muscle attached to the downstream part. One side of the rigid forepart is flat; the other side has a circular arc. The flat surface of the blade provides a reliable reference for setting the blade pitch during measurements. The muscle is sandwiched between two copper electrodes housed within the trailing end of the rigid part of the blade (figure 2(b)). The power supply to the electrodes is run through the hollow shaft (figure 2(c)), driving the propulsor.

Reinforced-type ionic polymer composite membrane artificial muscles, named MS-417 and MS-424, are used. The muscle end is sandwiched between two flat electrodes. When a voltage difference is applied between the electrodes, the muscle becomes charged and deflects.[10] It was observed that the muscle deflections were not equal on both sides. One side of the muscle was relatively rough and the other side was smooth. Presumably, the charge density on the surfaces was unequal, which led to a difference in deflection.
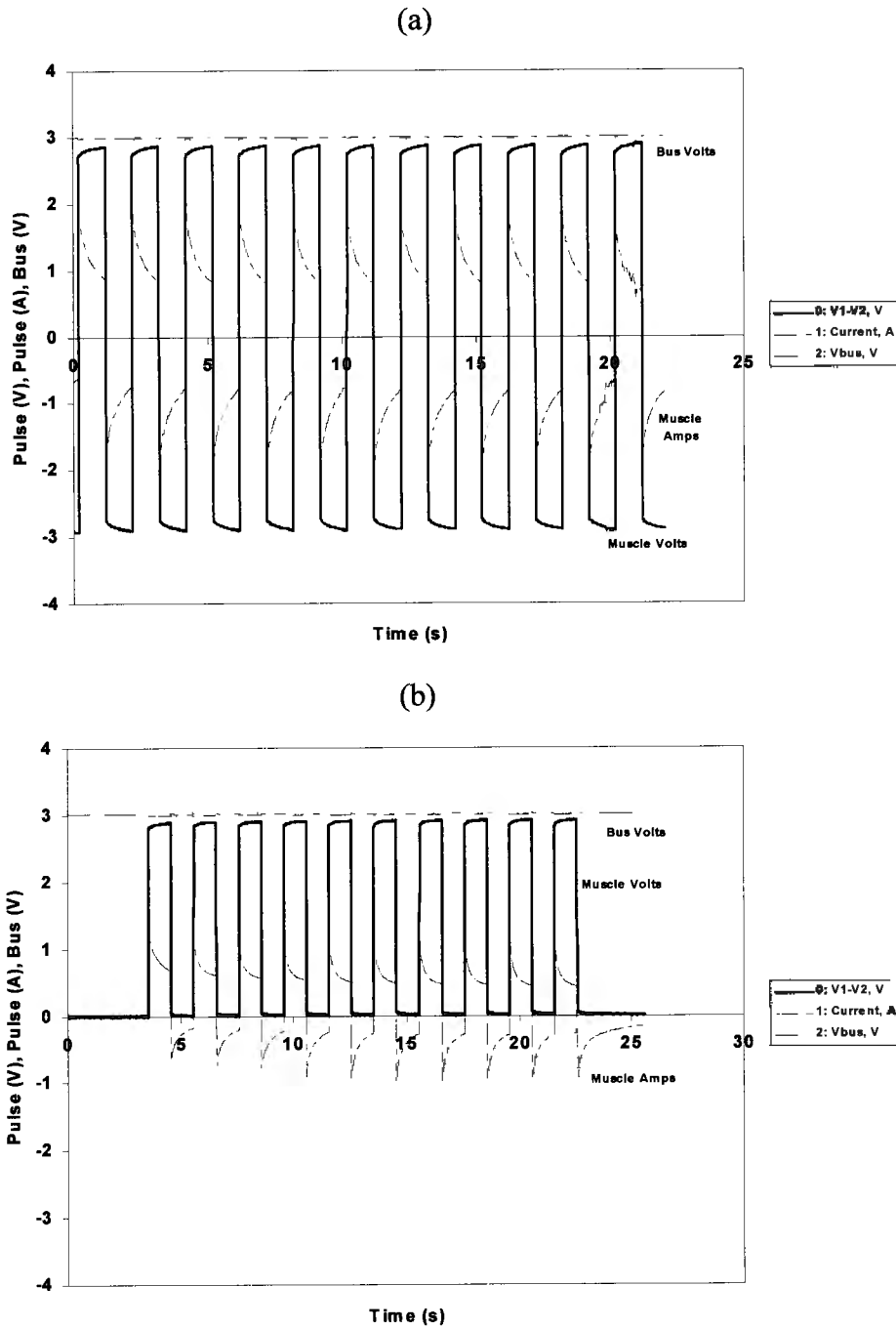
A power supply and digital controller were used to power the muscles. As shown in figure 3, any one of the following three voltage pulse forms could power the muscles: bipolar, positively unipolar, and negatively unipolar. The figure also shows the pulse forms of the current and the bus voltage. The pulse forms, voltage level, frequency, and duty cycle may be chosen on a computer monitor via "hot keys."

The various kinds of deflection that could be achieved are shown in figures 4 and 5. Figure 4 shows the deflections for a static blade, while figure 5 shows the deflections for a rotating blade. Figure 5 is included as evidence that the muscles remain deflected under the loading of the flow. The pressure difference across the rotating propulsor blade would tend to affect the blade deflection. An order of magnitude estimate of the potential difference that needs to be applied to null the unwanted extent of the blade deflection effect may be obtained by oscillating the muscles in still water, as shown in the video. Any reduction of deflection due to pressure difference across the muscle can be compensated by a higher applied potential difference across the electrodes.

Figure 2. Details of Biomimetic Propulsor: (a) End View of Blade with Artificial Muscle, (b) Plan View of Blade in (a), and (c) Experimental Setup of Propulsor Assembly in Water-Filled Box with Motor Drive and Load Cell (All measurements in millimeters.)

(a)

(b)

*Figure 3. Pulse Forms: (a) Bipolar, (b) Positive Unipolar, and (c) Negative Unipolar
(Muscle: MS-417 with cloth backing; motion of muscle: (a) predominantly large amplitude
oscillations from flat to large cambering; (b) predominantly flattens with minor oscillations;
(c) predominantly cambered with minor oscillations (no bubbling, 3 V, 1 Hz, duty cycle 50%).)*

5

(c)
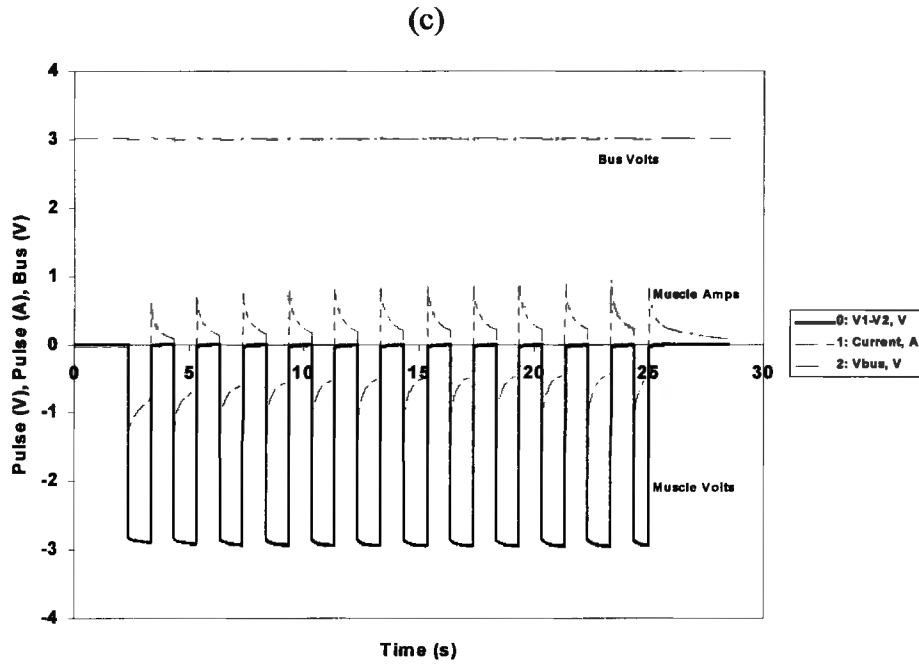
***Figure 3. Pulse Forms: (a) Bipolar, (b) Positive Unipolar, and (c) Negative Unipolar
(Muscle: MS-417 with cloth backing; motion of muscle: (a) predominantly large amplitude
oscillations from flat to large cambering; (b) predominantly flattens with minor oscillations;
(c) predominantly cambered with minor oscillations (no bubbling, 3 V, 1 Hz, duty cycle 50%).)
(Cont'd)***

6

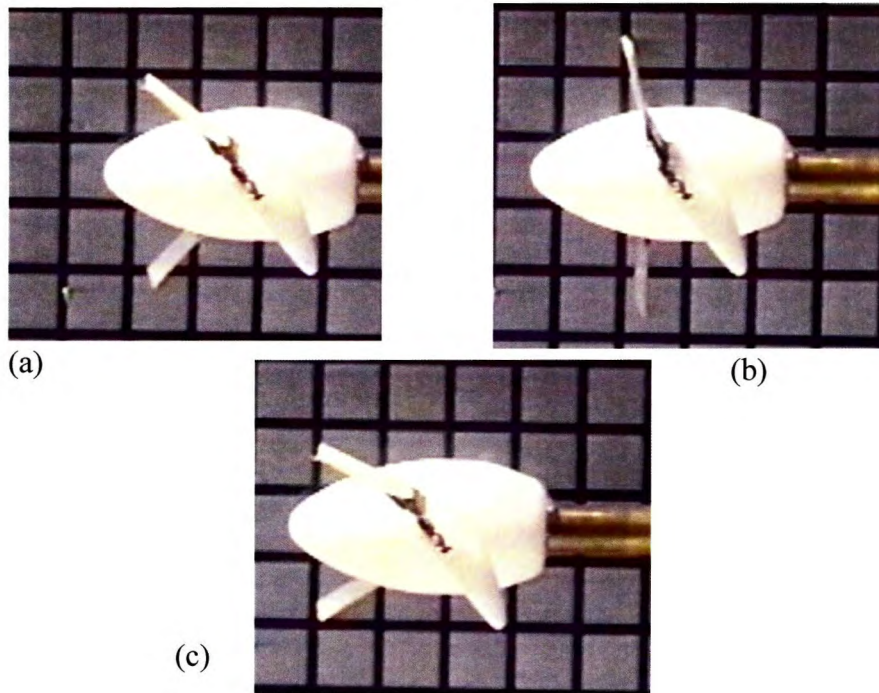*Figure 4. Cambering of Blade Muscle with Non-Rotating Propulsor (Input pulse forms and nature of cambering are as follows: (a) bipolar: muscle is flat, (b) positive unipolar: muscle is cambered negatively; negative lift – reverse thrust, and (c) negative unipolar: muscle is cambered positively; positive lift – forward thrust. Power supply to muscles: 100 Hz and 7 V; high frequency leads to cambering without oscillation and bubbles (1-cm x 1-cm grid).)*
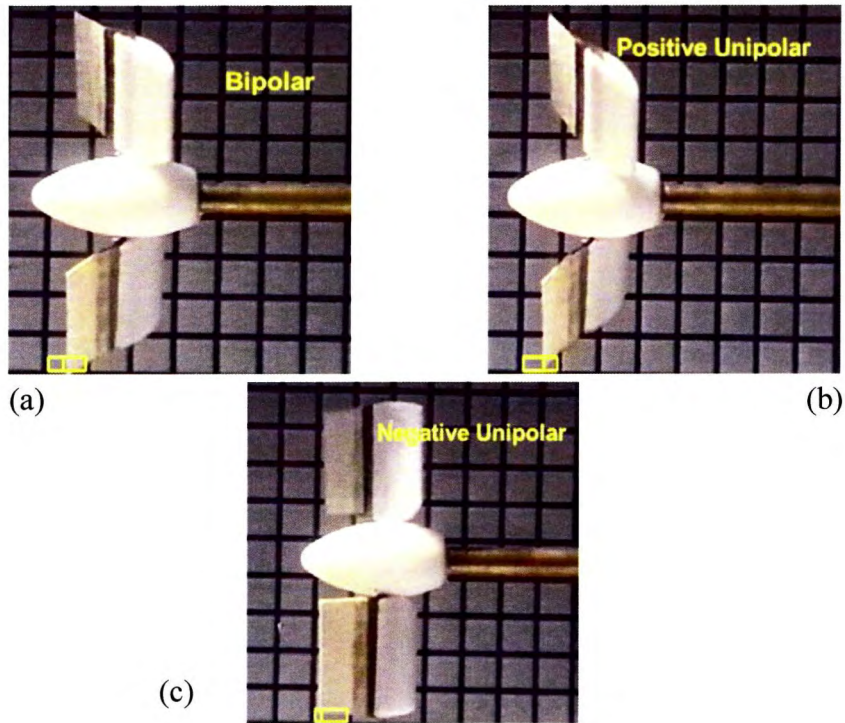
Figure 5. Photographs of Rotating Propulsor: (a) Bipolar, (b) Positive Unipolar, and (c) Negative Unipolar (Stills from video[8] indicate cambering of blade muscles during rotation. Notice trailing edge displacement with respect to the marked box during rotation; this displacement indicates that the muscle is staying cambered during rotation.)

The three kinds of deflections shown are obtained by the three kinds of pulse forms. However, the muscle could be purely cambered, purely oscillated, or a combination of the two. Cambering is achieved by means of controlling the voltage level, while oscillation is achieved by controlling the frequency of the pulse form. A low frequency, roughly in the range of 1 Hz to 10 Hz, produced an oscillation, while a frequency near 100 Hz produced no oscillation. The applied voltage produces a distribution of an electrical charge on the surface of the muscle. Normally, bubbles form on the muscle surface above 3 V. However, a higher frequency generally tended to suppress such bubble formation somewhat beyond 3 V. An encapsulated muscle sheet will not produce any bubble; therefore, this is not a long-term issue.

Figure 4 shows that muscles can be used to increase cambering to increase lift force, or even be cambered negatively, which presumably leads to a thrust reversal. The muscles start moving immediately after they are powered; however, it may take several seconds to reach their steady-state deflection.

3.2 EXPERIMENTAL SETUP

Figure 2(c) schematically shows the experimental setup. The propulsor is housed in a water-filled box with dimensions of 295 mm x 150 mm x 150 mm. To avoid degradation of performance of the electrodes and the muscle material, purified de-ionized water was used. This would not be a drawback in the future because the muscles can be encapsulated in de-ionized water and the electrodes can be made of platinum and made integral to the muscles. These improvements were considered non-essential for the purposes of the present hydrodynamic experiment. The tip-to-tip diameter of the propulsor is 77 mm. The drive shaft is hollow, and the muscle power cables run through it to a slip ring located outside of the box. The propulsor and drive shaft float. Before the propulsor was driven, it was slid back upstream and made no contact with the load cell. After the drive starts turning and thrust is produced, the propulsor moves freely downstream and pushes against a load cell situated just outside of the box. A Nano load cell, manufactured by ATI, Inc., has been used for thrust measurement. The force and moment measurements are 12 N and 0.12 N/m, respectively; the size of the load cell is 17 mm in diameter and 14.5 mm in height. This is a six-component load cell with monolithic beam construction. Silicon strain gauges are built on the beams. The resolution is 0.013 N for thrust measurement.

A personal computer (PC) was used to operate the load cell controller. Another PC was used for the controller of the muscle power supply. A third main PC was used to collect data from the two PCs, and to process and then plot the data.

3.3 BASELINE MEASUREMENTS

The measurements of time-averaged thrust for varying rotational speed for an inactive muscle are shown in figure 6. The mean is an rpm-squared trend, as it should be. The Reynolds number, based on chord and tip velocity, is $1.43 \times 10^4 \leq Re_c \leq 7.16 \times 10^4$ in the range of

$100 \leq \text{rpm} \leq 500$. The uncertainty in thrust measurement is large at very low values of rpm. Future experiments of turning the muscle on and off should be conducted at higher values of rpm; the result should yield less uncertainty in thrust measurement. In any case, the present diagnostic involves measurement of changes in thrust between two states, namely, when the muscles are deflected and not deflected. In such situations, the absolute accuracy of the thrust values is less important.
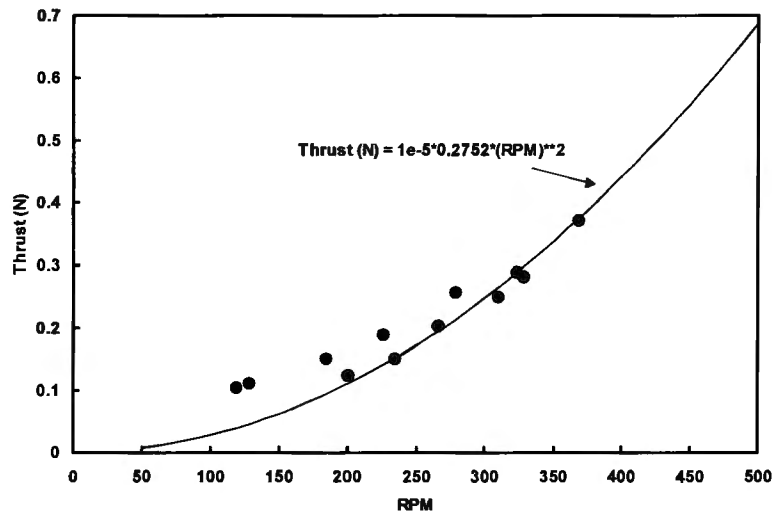
Figure 6. Comparison of Measurements of Time-Averaged Thrust with rpm-Squared Trend (Pitch is 73°, muscles are installed but not active, and two-bladed propulsor is used.)

To verify that the magnitudes of thrust measurements were reasonable, an order of magnitude calculation was performed to determine the expected thrust. Nondimensionalized $B_p - \delta$ design curves (relating horsepower to shaft speed) were used for the well-known and documented Series B set of propellers developed by the Netherlands Ship Model Basin at Wageningen. The B2.38 screw was chosen,[11] as its configuration (number of blades and expanded area ratio) was most similar (but not identical) to the experimental one. The following standard parameters were used to characterize the propeller:

V_A = speed of advance, meters per second,

n = shaft speed (rotations per second),

D = maximum propeller diameter in meters,

$R = D/2$,

J = advance coefficient, $J = \dfrac{V_A}{nD}$,

ϕ = pitch angle,

10

P = pitch for a given radius r, $P = 2\pi r \tan\phi$,
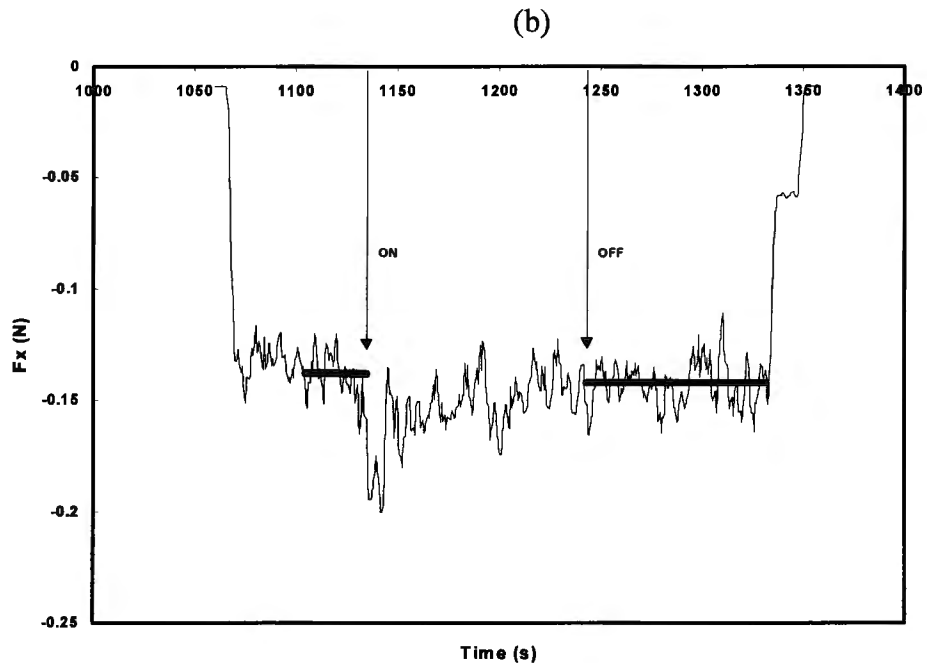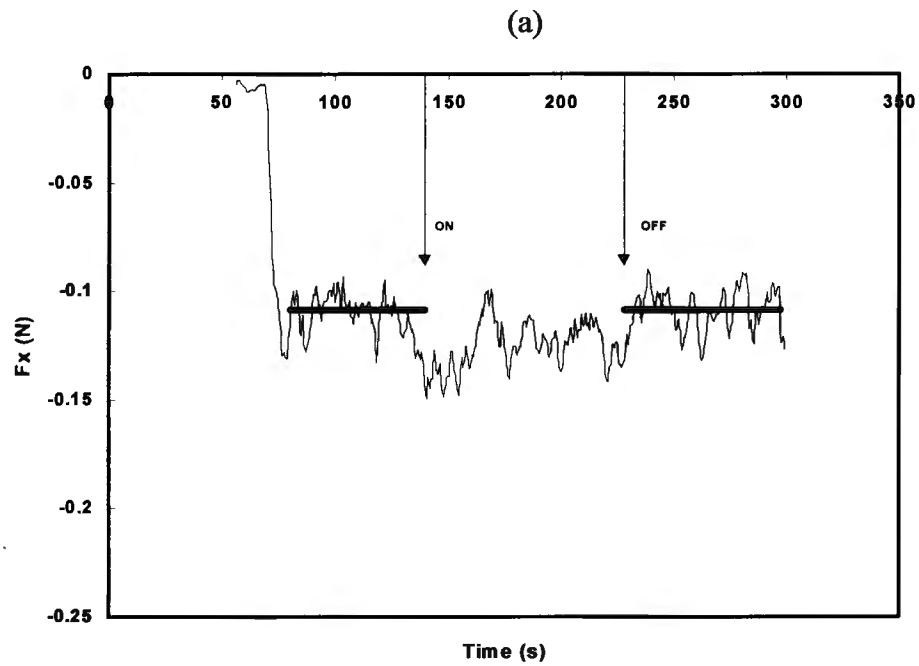
s_R = slip ratio, $s_R = 1 - \dfrac{J}{P/D}$,

A_e/A_0 = expanded area ratio, $A_e/A_0 = \dfrac{\text{expanded area of all blades}}{\pi R^2}$.

Using P/D of the test propeller at the characteristic radius $r = 0.7R$, and assuming s_R to be 25% at design J, it was determined using the design curves that approximately 0.3 N of thrust would be produced by a well-designed, two-bladed propeller operating at design J and 412 rpm. Its bollard pull (defined as the thrust produced when there is no speed of advance, i.e., $J = 0$, as in the experiment) is a small multiple of this value, depending on the design. The measured bollard pull of 0.45 N is therefore well within the expected value for an admittedly non-optimal design. In other words, as per the model, the pull is 4 x 0.3 N, while the measured value is 0.45 N. This is a reasonable order of magnitude agreement. The differences between the shape of the Series B blades and the biomimetic blades, and the fact that the current experiments were run in a relatively small enclosure, would both tend to decrease the expected thrust.

3.4   RESULTS

Thrust measurements were carried out to determine thrust enhancement due to active cambering, i.e., cambering of the muscles on demand, while the propulsor had been turning at a certain rpm. These measurements were carried out by turning the blade muscles off and on to determine the changes, and are shown in figure 7 for three values of rpm, namely, 325, 420, and 520. The flat pressure side of the blades was set to a pitch angle of zero degree to minimize the thrust produced by the propulsor and to maximize the relative effect of the blade cambering, which made detection of the effect of cambering on thrust easier than for a case with a large angle of pitch. The pulse frequency was 1 Hz, which led to both cambering and oscillation. Previous experience indicates that the electroactive muscle sheets do not deflect equally between one pulse cycle and another, and there may be some hysteresis. Thrust response to muscle powering is practically immediate (O(s)). There is, roughly, a 15% increase in thrust when the muscles are cambered.

The significance of the result can be understood in the following manner. A controllable lift (controllable pitch and camber) propulsor producing 15% additional thrust, compared to a similar conventional propulsor at the same rpm, can be operated at a 7% lower rpm to produce the same thrust. This could lead to approximately a 1-dB reduction in directly radiated blade tonal noise due to decreased flow velocity over the blade sections.

(a)

(b)

Figure 7. Comparison of Thrust Signature During Active Cambering Using a Two-Bladed Propulsor (Values of rpm are (a) 325, (b) 420, and (c) 520. Negative Fx indicates positive thrust. Muscle is MS-417 with cloth backing, power is 3 V, 1 Hz (no bubbles are produced during these measurements), and pulse is negative unipolar, producing positive cambering.)

(c)
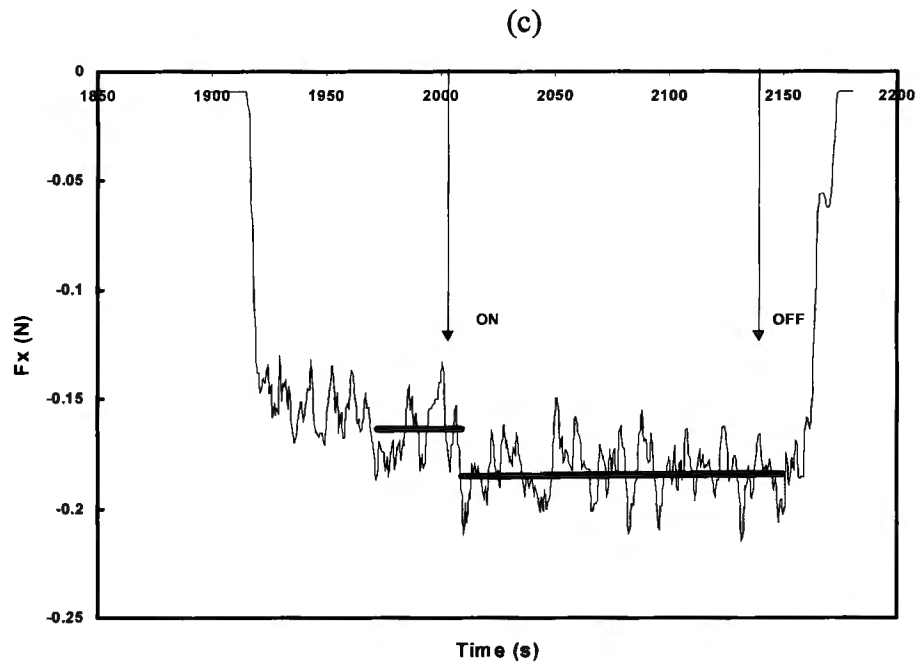
Figure 7. Comparison of Thrust Signature During Active Cambering Using a Two-Bladed
Propulsor (Values of rpm are (a) 325, (b) 420, and (c) 520. Negative Fx indicates positive
thrust. Muscle is MS-417 with cloth backing, power is 3 V, 1 Hz (no bubbles are produced
during these measurements), and pulse is negative unipolar, producing positive cambering.)
(Cont'd)

4. CONCLUSIONS

An attempt has been made in this report to develop a strategy for the reduction of noise in small underwater vehicles. Modeling has been carried out which suggests that hydrodynamic strategies for lift enhancement, leading to lower rotational speed, is such a route. Unsteady hydrodynamic mechanisms of lift production present in certain swimming and flying animals may be suited for application to propulsor blades, which would require the availability of an active blade cambering technology. Using recently developed electroactive polymeric muscles, the potential of such a digitally amenable technology has been demonstrated on a small laboratory propulsor. The value of active cambering may be in the improvement of propulsor and noise performance in off-design (off-cruise) conditions, such as maneuvering.

APPENDIX
MECHANICS OF PROPULSOR NOISE

This appendix provides an examination of the dependence of generated noise power on propulsor rotational speed. The following treatment is derived from the one developed in Ross.[9] Throughout the appendix, appropriate linearizing assumptions have been made, including compactness and the "acoustic assumption," in which physical quantities may be expressed as sums of steady-state and fluctuating values; i.e., for the general quantity A, position coordinates x, y, z, time t, and period T,

$$A(x,y,z,t) = A_0(x,y,z) + A'(x,y,z,t), \tag{A-1}$$

$$A_0 = \frac{1}{T}\int_0^T A\,dt . \tag{A-2}$$

A governing equation for sound generation[12] can be expressed in tensor notation as

$$\nabla^2 p' - \frac{1}{c_0^2}\ddot{p}' = -\dot{q}' + \nabla \cdot \vec{f}' - \frac{\partial \tau'_{ij}}{\partial x_i \partial x_j} , \tag{A-3}$$

where p', q', $\vec{f}'$, and τ'_{ij} are the fluctuating components of pressure, mass, force, and the turbulent stress tensor, respectively; c_0 is sound speed, and the dots represent partial derivatives with respect to time. The three terms in the right-hand side of equation (A-3) represent noise due to fluctuating volumes, fluctuating forces, and turbulence, respectively.

A.1 FLUCTUATING VOLUMES

The example of noise due to fluctuating volumes relevant to propulsors is from cavitation. It can be shown that the sound power due to this mechanism is proportional to the fourth power of blade-tip speed. Normally, it is assumed that torpedo and submarine propulsors will be operating in regimes where cavitation does not occur; therefore, fluctuating volume noise will not be considered further.

A.2 FLUCTUATING FORCES

The operation of a propulsor in a circumferentially non-uniform wake produces fluctuating thrust and side forces. This causes direct acoustic dipole radiation into the surrounding fluid, which is independent of any resultant structural vibration. Usually, the most significant consequence of any propulsor blade vibration is its transmission to the attached structures and subsequent re-radiation. The modeling of structural vibrations is complex and beyond the

scope of this report; the focus here will remain on direct radiation. Fortunately, reduction of the fluctuating forces that cause directly radiated sound also attenuates the structural forcing functions and the resultant indirect sound radiation.

The following analysis is for thrust but can be applied to other force components. Circumferential variation in the in-flow causes oscillations in thrust at multiples of the blade frequency f:

$$f = mBn,$$ (A-4)

where m is the order of the harmonic, B is the number of blades, and n is the speed in rotations per second. The non-dimensionalized unsteady thrust $\tilde{C}_{T_m}$ for the m-th harmonic is expressed as

$$\tilde{C}_{T_m} = \frac{\tilde{T}_m}{\rho_0 n^2 D^4},$$ (A-5)

where $\tilde{T}_m$ is the fluctuating component of thrust, ρ_0 is the steady-state fluid density, and D is the diameter. For large wavelengths compared to the body, i.e., $kD < 1$, where

$$kD = \frac{2\pi m B n D}{c_0},$$ (A-6)

the acoustic power W_{ac} can be derived as

$$W_{ac} = \frac{m^2 B^2}{3c_0^3} \rho_0 n^6 D^8 \left(\tilde{C}_{T_m}\right)^2.$$ (A-7)

Acoustic power is therefore proportional to the sixth power of blade-tip speed $n\pi D$. Empirical evidence (the phenomenon of "trailing edge singing" of the blades of some tactical-scale vehicle propulsors), along with theory,[13] have shown that for $kD > 2$, acoustic power is actually proportional to the fifth power of blade-tip speed.

A.3 TURBULENCE

The fluctuating component of the turbulent stress tensor τ'_{ij} is given by

$$\tau'_{ij} = \left(\rho v_i v_j\right)' + \left(p'_{ij} - p'\delta_{ij}\right) + \left(p' - c_0^2 \rho'\right)\delta_{ij},$$ (A-8)

where ρ is density, v_i is the i-th component of particle velocity, p_{ij} is a pressure stress tensor, and δ_{ij} is the Kronecker Delta. The terms in the right-hand side of the equation represent fluctuating shear stresses associated with, respectively, turbulent fluid motions, viscous stresses, and heat conduction and/or nonlinearity. Only the first is of significance in liquid flows, and can be approximated to the first order by

$$\tau'_{ij} = 2\rho_0 U_0 u'_i, \tag{A-9}$$

where U_0 is the flow speed and u'_i is the i-th component of the fluctuating hydrodynamic velocity. This leads to an expression for the sound generated by turbulence, assuming a small source region compared to the sound wavelength:

$$p' = \frac{\rho_0 U_0}{2\pi r} \frac{\partial^2}{\partial x_i \partial x_j} \int_V u'_i \, dV, \tag{A-10}$$

where V is the source volume. This sound is quadruple in nature; its power is proportional to the sixth power of the flow speed.

REFERENCES

1. C. P Ellington, "The Aerodynamics of Hovering Insect Flight: IV. Aerodynamic Mechanisms," *Philosophical Transactions of the Royal Society of London Series B*, vol. 305, 1984, pp. 79–113.

2. M. H. Dickinson, F. Lehmann, and S. P. Sane, "Wing Rotation and the Aerodynamic Basis of Insect Flight," *Science*, vol. 284, 1999, pp. 1954–1960.

3. P. R. Bandyopadhyay, J. M. Castano, J. Q. Rice, R. B. Philips, W. H. Nedderman, and W. K. Macy. "Low-Speed Maneuvering Hydrodynamics of Fish and Small Underwater Vehicles," *ASME Journal of Fluids Engineering*, vol. 119, 1997, pp. 136–144.

4. P. R. Bandyopadhyay, S. Singh, and F. Chockalingam, "Biologically Inspired Bodies Under Surface Waves, Part 2: Theoretical Control of Maneuvering," *ASME Journal of Fluids Engineering*, vol. 121, no. 2, 1999, pp. 479–487.

5. W. H. Nedderman, P. R. Bandyopadhyay, and J. Dick, "Biologically-Inspired Bodies Under Surface Waves. Part 1: Load Measurements," *ASME Journal of Fluids Engineering*, vol. 121, no. 2, 1999, pp. 469–478.

6. P. R. Bandyopadhyay, "Emerging Approaches to Flow Control in Hydrodynamics," *38th IEEE Conference on Decision and Control*, Tempe, AZ, 1999, pp. 2845–2850.

7. P. R. Bandyopadhyay, J. M. Castano, W. H. Nedderman, and M. J. Donnelly, "Experimental Simulation of Fish-Inspired Unsteady Vortex Dynamics on a Rigid Cylinder," *ASME Journal of Fluids Engineering*, vol. 122, 2000, pp. 219–238.

8. P. R. Bandyopadhyay, J. M. Castano, W. H. Nedderman, and M. J. Donnelly, "Biomimetics Research at NUWC," Video (edited), Naval Undersea Warfare Center Division, Newport, RI, 2000.

9. D. Ross, *Mechanics of Underwater Noise*, Peninsula Publishing, Los Altos, CA, 1987.

10. M. Shahinpoor, "Ion-Exchange Polymer-Metal Composites as Biomimetic Sensors and Actuators–Artificial Muscles," *Proceedings of the Special Session on Bio-Engineering Research Related to Autonomous Underwater Vehicles*, 10th International Symposium on Unmanned, Untethered Submersible Technology, Organized by Autonomous Undersea Systems Institute, Durham, NH, 10 and 11 September 1997, pp. 62–85.

11. F.H. Todd, "Resistance and Propulsion," *Principles of Naval Architecture*, Chapter 7, Society of Naval Architecture and Marine Engineers, 1967, p. 413.

12. M. J. Lighthill, "On Sound Generated Aerodynamically: 1. General Theory", *Proceedings of the Royal Society*, vol. A211, 1952, p. 1107.

13. M. V. Lawson, "Theoretical Analysis of Compressor Noise," *Journal of the Acoustical Society of America*, vol. 47, 1970, pp. 371–385.

INITIAL DISTRIBUTION LIST

Addressee	No. of Copies
Naval Surface Warfare Center/Carderock Division (J. Fein, D. Hess, S. Jessup, M. Wilson)	4
Office of Naval Research (ONR-33 -- S. Lekoudis, ONR-34 -- H. Guard, ONR-342 -- W. Vaughan, H. Bright, R. Gisiner, ONR-333 -- T. McMullen, P. Purtell, K. Ng, R. Joslin, ONR-334 – J. Muench)	10
University of Arizona (E. Kerschen)	1
Massachusetts Institute of Technology, Mechanical Engineering Dept. (I. Hunter)	1
Massachusetts Institute of Technology, Dept. of Oceanography (M. Triantafyllou)	1
Westchester University (F. Fish)	1
University of Illinois/Urbana-Champagne (R. Adrian, W. Phillips)	2
Virginia Polytechnic Institute (D. Telionis, R. Simpson)	2
University of Michigan (G. Faeth, P. Webb)	2
Yale University (K. Sreenivasan)	1
University of Houston (F. Hussain)	1
UCLA (J. Kim)	1
Stanford University (P. Moin, B. Cantwell)	2
Cambridge University/UK (C. Ellington, A. Dowling)	2
Princeton University (A. Smits, G. Brown)	2
Iowa Institute of Hydraulic Research (V. Patel)	1
Defense Advanced Research Projects Agency (A. Rudolf)	1
Anteon Corporation (J. Grant, J. Uhlman)	2
NASA Langley Research Center (D. Bushnell)	1